

# Mapping of the Functional Interconnections Between Thalamic Reticular Neurons Using Photostimulation

Ying-Wan Lam, Christopher S. Nelson and S. Murray Sherman

*J Neurophysiol* 96:2593-2600, 2006. First published Jul 19, 2006; doi:10.1152/jn.00555.2006

**You might find this additional information useful...**

---

This article cites 29 articles, 12 of which you can access free at:

<http://jn.physiology.org/cgi/content/full/96/5/2593#BIBL>

Updated information and services including high-resolution figures, can be found at:

<http://jn.physiology.org/cgi/content/full/96/5/2593>

Additional material and information about *Journal of Neurophysiology* can be found at:

<http://www.the-aps.org/publications/jn>

---

This information is current as of October 24, 2006 .

# Mapping of the Functional Interconnections Between Thalamic Reticular Neurons Using Photostimulation

Ying-Wan Lam, Christopher S. Nelson, and S. Murray Sherman

*Department of Neurobiology, Pharmacology and Physiology, The University of Chicago, Chicago, Illinois*

Submitted 24 May 2006; accepted in final form 18 July 2006

**Lam, Ying-Wan, Christopher S. Nelson, and S. Murray Sherman.** Mapping of the functional interconnections between thalamic reticular neurons using photostimulation. *J Neurophysiol* 96: 2593–2600, 2006. First published July 19, 2006; doi:10.1152/jn.00555.2006. The thalamic reticular nucleus is strategically located in the axonal pathways between thalamus and cortex, and reticular cells exert strong, topographic inhibition on thalamic relay cells. Although evidence exists that reticular neurons are interconnected through conventional and electrical synapses, the spatial extent and relative strength of these synapses are unclear. To address these issues, we used uncaging of glutamate by laser-scanning photostimulation to provide precisely localized and consistent activation of reticular cell bodies and dendrites in an *in vitro* slice preparation from the rat as a means to study reticulo-reticular connections. Among the 47 recorded reticular neurons, 29 (62%) received GABAergic axodendritic input from an area immediately surrounding each of the recorded cell bodies, and 8 (17%) responded with depolarizing spikelets, suggesting inputs through electrical synapses. We also found that TTX completely blocked all evoked IPSCs, implying that any dendrodendritic synapses between reticular cells either are relatively weak, have no nearby glutamatergic receptors, or are dependent on back-propagation of action potentials. Finally, we showed that the GABAergic connections between reticular cells are weaker than those from reticular cells to relay cells. Our results suggest that the GABAergic axodendritic synapse is the dominant form of reticulo-reticular connectivity, and because they are much weaker than the reticulo-relay cell synapses, their functional purpose may be to regulate the spatial extent of the reticular inhibition on relay cells.

## INTRODUCTION

The thalamic reticular nucleus is strategically located in the axonal pathways between thalamus and cortex, and reticular cells receive inputs from collaterals of both thalamocortical and corticothalamic axons. These reticular cells, in turn, provide a GABAergic, inhibitory input to thalamic relay cells (reviewed in Sherman and Guillery 2006). These relationships allow the thalamic reticular nucleus to play a crucial role in the thalamic relay of information to cortex (reviewed in Guillery and Harting 2003; Guillery et al. 1998; Pinault 2004; Sherman and Guillery 2006).

To more completely understand how the thalamic reticular nucleus functions to affect thalamocortical relays, we need a better appreciation of its intrinsic organization. The thalamic reticular nucleus was once thought to be diffusely organized, but it is now clear that there is considerable topography in its connections (Crabtree 1992a,b, 1996; Lam and Sherman 2005). It is also clear that there is interconnectivity among

reticular cells and that this interconnectivity can play a key role not only in determining the extent of inhibitory influences on relay cells, but it is also critical to the establishment of various rhythms that can occur in thalamocortical circuits (reviewed in Fuentealba and Steriade 2005).

These intrareticular connections seem to take three forms: axodendritic synapses, from collaterals of axons that innervate relay cells (Sanchez-Vives et al. 1997; Shu and McCormick 2002; Zhang et al. 1997); dendrodendritic synapses (Deschênes et al. 1985; Pinault et al. 1997; Yen et al. 1985); and electrical synapses through gap junctions (Landisman and Connors 2005; Landisman et al. 2002). While these forms of interconnectivity seem well established, the extent and strength of the interconnections remain unclear, especially for the chemical synapses involving GABA (Landisman and Connors 2005; Landisman et al. 2002; Pinault et al. 1995a,b). Our goal in this experiment was to use the technique of local activation of reticular cells by the method of uncaging of glutamate through laser photostimulation to determine the extent and strength of these local intrareticular connections. We studied these connections in the region of the rat's thalamic reticular nucleus associated with the relay of somatosensory information.

## METHODS

### *Preparation of thalamic slices*

All animal procedures followed the animal care guidelines of the University of Chicago. All experiments were performed on thalamic slices taken from young rats (10–12 days postnatal, except for those in relay cells of the lateral geniculate nucleus, which were 15–20 days postnatal). To obtain the slices, each animal was deeply anesthetized by inhalation of isoflurane, and its brain was quickly removed and chilled in ice-cold artificial cerebrospinal fluid (ACSF), which contained (in mM) 125 NaCl, 3 KCl, 1.25 NaH<sub>2</sub>PO<sub>4</sub>, 1 MgCl<sub>2</sub>, 2 CaCl<sub>2</sub>, 25 NaHCO<sub>3</sub>, and 25 glucose. Tissue slices (400  $\mu$ m) were cut using a vibrating tissue slicer, transferred to a holding chamber containing oxygenated physiological saline maintained at 30°C, and incubated for  $\geq 1$  h before recording. The slices were either cut in the horizontal plane or in the plane appropriate for an intact thalamocortical slice (Agmon and Connors 1991; Reichova and Sherman 2004). Slices containing the lateral geniculate nucleus (Fig. 4) were prepared in a similar way and cut in coronal sections.

### *Physiological recording*

Whole cell recordings were performed using a visualized slice setup (Cox and Sherman 2000; Lam and Sherman 2005). Recording pipettes were pulled from borosilicate glass capillaries and had tip

Address for reprint requests and other correspondence: S. M. Sherman, Dept. of Neurobiology, Pharmacology and Physiology, Univ. of Chicago, 947 E. 58th St., MC 0926, 316 Abbott, Chicago, IL 60637 (E-mail: msherman@bsd.uchicago.edu).

The costs of publication of this article were defrayed in part by the payment of page charges. The article must therefore be hereby marked "advertisement" in accordance with 18 U.S.C. Section 1734 solely to indicate this fact.

resistances of 4–8 M $\Omega$  when filled with solution (termed hereafter the pipette solution). For most cells, this solution was (in mM) 117 Cs-gluconate, 13 CsCl, 2 MgCl<sub>2</sub>, 10 HEPES, 2 Na<sub>2</sub>-ATP, and 0.3 Na-GTP. Biocytin (0.4%) was included in the pipette in a few experiments for histological characterization of the reticular neurons. We typically recorded in voltage-clamp mode, but occasionally used current-clamp recordings. In most cases involving voltage-clamp recording, the K<sup>+</sup> channel blocker, Cs<sup>+</sup>, was used in the pipette solution to suppress  $I_{K_{leak}}$  and thus help maintain the holding voltage at 0 mV. In other cases, we replaced the Cs<sup>+</sup> with K<sup>+</sup> or Na<sup>+</sup> (final concentration in mM: 135 K-gluconate, 7 NaCl, 2 MgCl<sub>2</sub>, 10 HEPES, 2 Na<sub>2</sub>-ATP, and 0.3 Na-GTP). The pH of the pipette solution was adjusted to 7.3 with CsOH (or KOH in cases where we used K<sup>+</sup> or Na<sup>+</sup> instead of Cs<sup>+</sup>) or gluconic acid, and the osmolality was 280–290 mOsm.

Recordings were obtained using an Axopatch 200B (Axon Instruments, Foster City, CA). The amplitudes of IPSCs were maximized by holding the cells at 0 mV (Cox and Sherman 2000; Lam and Sherman 2005). The access resistance of the cells was constantly monitored throughout the recordings (>1 h for most experiments), and recordings were limited to neurons with a stable access of <30 M $\Omega$  throughout the experiment. Effects of antagonists (SR 95531, CGP 46381, TTX, and carboxolone) were assayed by bath-application of the drugs. The GABA antagonists SR 95531 (gabazine) and CGP 46381 were purchased from Tocris (Ellisville, MO). All the other chemicals were purchased from Sigma-Aldrich (St. Louis, MO).

### Photostimulation

We used our previously described methods for photostimulation (Lam and Sherman 2005). Data acquisition and photostimulation were controlled by a program written in Matlab (MathWorks, Natlick, MA) developed in the laboratory of Karel Svoboda (Shepherd et al. 2003). Nitroindolyl (NI)-caged glutamate (Sigma-RBI; Canepari et al. 2001) was added to recirculating ACSF to a concentration of 0.39 mM during recording. Focal photolysis of the caged glutamate was accomplished by a pulsed UV laser (355 nm wavelength, frequency-tripled Nd:YVO<sub>4</sub>, 100-kHz pulse repetition rate, DPSS Laser, San Jose, CA). Figure 1A is a schematic illustration of the optics: the laser beam was directed into the side port of an Olympus microscope (BX50WI) using UV-enhanced aluminum mirrors (Thorlabs, Newton, NJ) and a pair of mirror galvanometers (Cambridge Technology, Cambridge, MA) and focused onto the brain slice using a low-magnification objective (4x0.1 Plan, Olympus). Angles of the galvanometers were computer controlled and determined the position stimulated by the laser. The optics was designed to generate a nearly cylindrical beam in the slice to keep the mapping two dimensional (Shepherd et al. 2003). The Q-switch of the laser and a shutter (LS3-ZM2, Vincent Associate, Rochester, NY) controlled the timing of the laser pulse for stimulation. A variable neutral density wheel (Edmund, Barrington, NJ) controlled the power of the laser at different levels during experiments by attenuating the intensity of the laser. A thin microscope coverslip in the laser path reflected a small portion of the laser onto a photodiode. The current output from this photodiode was amplified, acquired by the computer, and used to monitor the laser intensity during the experiment. Photodiode output was calibrated to laser power when we set up the optical equipment: the laser power at the back focal plane of the objective was measured using a power meter (Thorlabs).

Figure 1B is a photomicrograph taken during a typical experiment. The borders between the internal capsule, thalamic reticular nucleus, and dorsal thalamus are indicated in this and other illustrations with dotted lines; thus the zone between dotted lines in each illustration represents the thalamic reticular nucleus. A few threads of nylon filaments, attached to a platinum wire slice holder, were used to secure the thalamic slices in the recirculating bath. The distance between these filaments was large (~1 mm), and they were always carefully placed to avoid the area of recording and photostimulation (Fig. 1B)

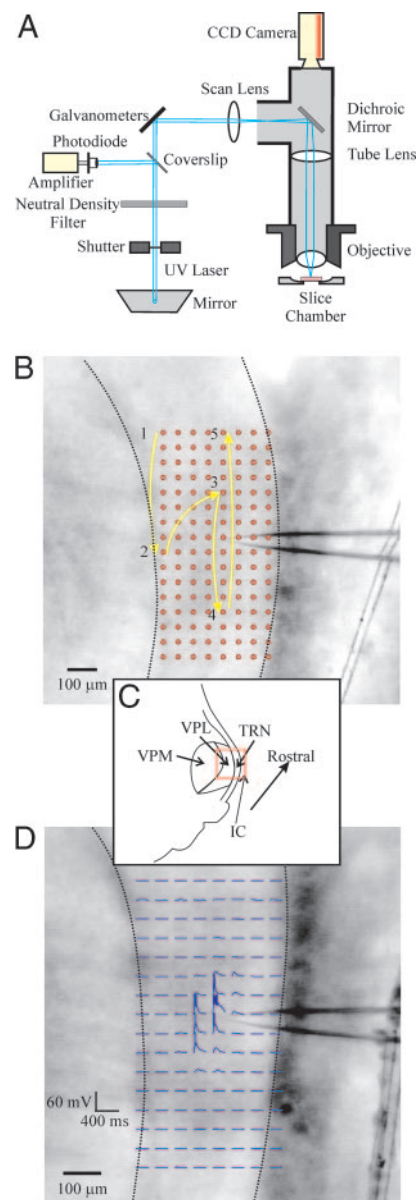


FIG. 1. Method for photostimulation. *A*: schematic diagram of the optics of the laser-scanning photostimulation setup used in this study. *B*: photomicrograph of the slice preparation superimposed with a diagram of photostimulation pattern. We recorded from neurons of the thalamic reticular nucleus in horizontal (shown here) or thalamocortical slices of rat. Semitransparent bands seen in this and other photomicrographs are threads used to tether the slice. Each red circle in the rectangular array indicates a location at which the laser is focused during the mapping trials. Spot locations are stimulated in a distributed manner, and positions of the 1st 5 trials are indicated. Dotted lines in this and other photomicrographs indicate borders of thalamic reticular nucleus, with ventral posterior lateral nucleus to the left and internal capsule to the right. *C*: anatomical relationships of relevant nuclei shown schematically at smaller scale (VPM, ventral posterior medial nucleus; VPL, ventral posterior lateral nucleus; TRN, thalamic reticular nucleus; IC, internal capsule). Area shown in photomicrographs in *B* and *D* is indicated by the red rectangle. *D*: spatial specificity of photostimulation. Responses of a neuron in current-clamp mode to photostimulation at 128 positions are arranged in an 8 × 16 matrix. In this example, photostimulation evoked action potentials in an elliptical area surrounding the soma of the recorded neuron. Laser power was 15 mW at the back focal plane of the microscope objective. As in *B*, dotted lines indicate position of thalamic reticular nucleus.

during experiments. The standard stimulation pattern for mapping the reticular input consisted of 128 positions in an  $8 \times 16$  array, with  $50 \mu\text{m}$  between adjacent rows and columns (Fig. 1B, red circles). To avoid receptor desensitization, local caged-glutamate depletion, and excitotoxicity, stimulation of these positions were arranged in a sequence that maximized the distance between consecutive trials (Fig. 1B). The light stimulus was 2 ms long, which consisted of 200 laser pulses. The time interval between photostimuli was 5 s. The laser power used (measured at the back-focal plane of the objective) ranged from 7 to 25 mW. We did not see any change of the recording quality during experiments that suggested damage from the photostimulation.

### Data analysis

Responses were analyzed using programs written in Matlab. For presentation of the data, traces of 200 ms recording immediately after the photostimulation were superimposed on a photomicrograph of the slice and recording pipette (see RESULTS). The photomicrographs were taken without using differential infrared-contrast (DIC) and therefore brain regions including an extensive fiber representation, such as the internal capsule or ventral posterior lateral nucleus, appeared dark because of the high contrast settings of the video camera as shown in a number of figures below. The above-mentioned traces were arranged into a  $8 \times 16$  array and placed where the laser was focused during the stimulation, so that the reticular area that projected to the recorded neuron could be visualized as that with a large upward current (IPSCs) in these traces. Differences between the IPSCs evoked were compared using Student's *t*-test.

## RESULTS

We recorded from a total of 47 neurons of the thalamic reticular nucleus. For 35 neurons, the slice was cut in the horizontal plane, and in the other 12, we used the plane appropriate for thalamocortical connections as described by Agmon and Connors (1991; see also Reichova and Sherman 2004). We saw no major differences resulting from the different planes of section.

### Spatial specificity of photostimulation

We were initially interested in the spatial extent of the region from which photostimulation could elicit direct depolarization of a cell. Figure 1C shows a typical experiment, showing the response in current clamp of a reticular neuron to photostimulation at the laser power commonly used (15 mW at the back focal plane of the microscope objective). Photostimulation of spots in a roughly elliptical region around the cell body elicited large depolarizations and long trains of action potentials. We estimated the size of the region from which direct responses were elicited in the recorded neuron by visually identifying traces with detectable depolarization; the average dimensions from a total of three experiments were  $233 \pm 76 \times 100 \pm 0$  (SD)  $\mu\text{m}$ , suggesting a high spatial specificity of photostimulation even with the relatively high laser powers we used.

### Response of reticular neurons to photostimulation within the thalamic reticular nucleus

The *middle column* of Fig. 2 shows 200 ms of the recorded responses immediately after photostimulation arranged in an  $8 \times 16$  array and superimposed on a photomicrograph of the slice at the location where the laser is focused. These responses are moderately enlarged in the *right column* in the area imme-

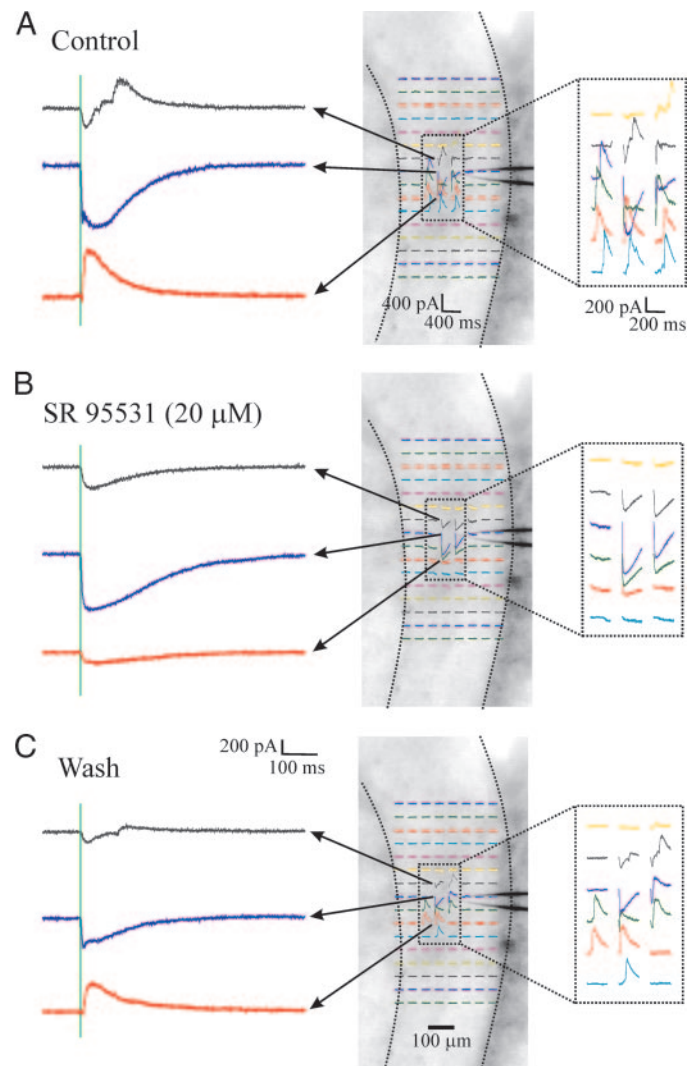


FIG. 2. Responses in voltage-clamp mode to direct photostimulation of reticular neuron. Laser power used in these experiments was 15 mW. *Middle column*: photomicrograph of slice preparation, and superimposed on it are responses to photostimulation at 128 positions, arranged in an  $8 \times 16$  array. Dotted lines indicate location of thalamic reticular nucleus. *Right column*: responses within dotted rectangles of *middle column* at a larger scale. *Left column*: at an even larger scale, recordings of selected trials indicated by arrows from *middle column*. *A*: control photostimulation, which evoked biphasic depolarization/hyperpolarization responses in an elliptical area surrounding the cell body. *B*: outward (hyperpolarizing) currents eliminated by application of GABA<sub>A</sub> antagonist, SR 95531. *C*: return of outward currents after washing out GABA<sub>A</sub> antagonist.

diately surrounding the soma, and the *left column* shows full traces at selected locations. As expected from the preceding paragraph, with voltage-clamp recording, photostimulation near the soma of reticular neurons evoked prominent inward currents (Fig. 2A, *left column*, blue trace). However, in 29 of the 47 (61%) recorded neurons, somewhat more eccentric photostimulation evoked biphasic responses that consisted of a late outward (hyperpolarizing) current after an early inward (depolarizing) current (Fig. 2A, *left column*, black trace). More eccentric photostimulation evoked an outward current with little or no preceding inward current (Fig. 2A, *left column*, red trace). The outward currents were judged to be GABAergic inhibitory postsynaptic currents (IPSCs) because they were

blocked by bath-application of the GABA<sub>A</sub> antagonist, SR95531 (Fig. 2*B*); this IPSC recovered after the drug was washed out (Fig. 2*C*). Because photostimulation specifically activates the soma or dendrites of a neuron, this GABAergic response could only come from the synaptic coupling between reticular neurons. For the other 18 reticular neurons, we could not detect any late outward or hyperpolarizing current (see DISCUSSION).

We recorded from seven cells using K<sup>+</sup> in the pipette solution (see METHODS). In six of these cells, we were able to detect a current response to photostimulation that was completely blocked by GABA<sub>A</sub> antagonist, SR 95531. Further application of CGP 46381, a GABA<sub>B</sub> antagonist, had no detectable effect on the remaining responses in four of these experiments.

As can be seen in the *right column* of Fig. 2, the region in which synaptic responses could be evoked by photostimulation generally consisted of a small elliptical area immediately around the recorded neuron. The region in which IPSCs could be evoked was visually identified, and the size was measured for each experiment. IPSCs were detected in 22 of 35 (63%) experiments using horizontal slices, and the areas measured  $366 \pm 21$  (SE)  $\mu\text{m}$  medio-laterally and  $180 \pm 11$   $\mu\text{m}$  dorso-caudally. IPSCs were detected in 7 of the 12 (58%) experiments using thalamocortical slices, and the average size of the areas in which they could be evoked was  $350 \pm 22$  and  $200 \pm 19$   $\mu\text{m}$ . The areas were not significantly different for the experiments carried out in the two different planes of sectioning (Student's *t*-test, *df* = 27, *P* > 0.68 for the long axis and *P* > 0.35 for the short axis).

#### Comparison of reticulo-reticular and reticular-relay cell synapses

We had previously used photostimulation to assess certain properties of the synapses between these reticular cells and relay cells of the ventral posterior lateral nucleus (Lam and Sherman 2005). After comparing those IPSCs with those evoked in this study, it seemed clear that the synaptic coupling between neighboring reticular neurons is weaker than that between reticular and relay neurons. Figure 3 provides a comparison of the two pathways, and Fig. 3, *A* and *B*, shows how data were selected for comparison. First, for reticulo-reticular IPSCs, we measured and averaged the peak values of the IPSCs evoked by photostimulation as described above on both sides  $\sim 100$   $\mu\text{m}$  mediolaterally from the recording site, where the IPSCs were large and the direct depolarization was relatively small (Fig. 3*A*, *left*, arrows for the photostimulation sites and red star for the recording site); these average IPSC amplitudes were plotted against the laser power used (Fig. 3, *C* and *D*,  $\Delta$ ). For comparison with our previously published results on the reticular to relay cell IPSCs, we include present data only from the 35 reticular cells (including those from which we failed to detect any evoked IPSCs) for which we used the same horizontal plane of sectioning as previously (Lam and Sherman 2005). Data from 52 relay neurons of the ventral posterior lateral nucleus were taken from Lam and Sherman (2005). The centroids (Fig. 3*B*, *left*, blue stars) of the reticular input footprint to these relay neurons were calculated as previously described (Lam and Sherman 2005). The peak values of the IPSCs evoked by photostimulation either at the

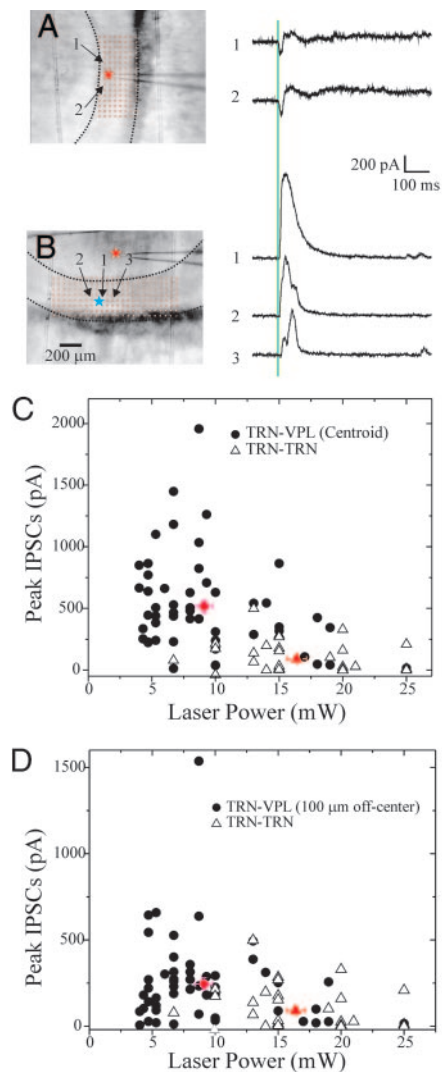


FIG. 3. Comparison of reticulo-reticular and reticular-relay cell synaptic activation. *A*: photomicrograph showing slice preparation and stimulation locations (*left*) and responses of reticular neuron (*right*) to reticular photostimulation at positions indicated by numbered arrows. Photostimulation positions are arranged at  $\sim 100$   $\mu\text{m}$  mediolaterally to each side of the recording site (red star). Peak inhibitory postsynaptic currents (IPSCs) of both traces were averaged for each cell thus studied for a single value, and these data are plotted in *C* and *D*. Laser power was 15 mW. *B*: photomicrograph (*left*) taken during an experiment in which we recorded from a relay cell (red star) in the ventral posterior lateral nucleus while stimulating the thalamic reticular nucleus (red circles). Footprint centroid of reticular input is calculated as previously described (Lam and Sherman 2005) and indicated with a blue star. Response (*right*) of relay cell to photostimulation at centroid (arrow 1) is shown in trace 1. For comparison with reticulo-reticular responses, we also evoked responses from photostimulation at positions marked by arrows 2 and 3, which were 100  $\mu\text{m}$  medially and laterally from the centroid, and these are shown on the *right* in traces 2 and 3. As in *A*, traces 2 and 3 for each cell were averaged to provide 1 value. Laser power was 8 mW. Dotted lines in *A* and *B* indicate borders of thalamic reticular nucleus. *C*: plot of peak IPSCs evoked by photostimulation vs. laser power. Responses of reticulo-reticular activation are plotted as open triangles, and those of peak reticular-relay cell responses to photostimulation at the reticular centroids are plotted as closed circles. Averages are shown as a red triangle for reticulo-reticular IPSCs and a red circle for reticular-relay cell IPSCs. Error bars indicate SE. *D*: plot of peak IPSCs vs. laser power as in *C*, except that data for relay cells are from photostimulation at points 100  $\mu\text{m}$  from reticular centroids.

centroid (Fig. 3*B*, left, arrow 1), and on both sides  $\sim 100 \mu\text{m}$  mediolaterally to the centroid (Fig. 3*B*, left, arrows 2 and 3) were measured and plotted in Fig. 3, *C* and *D*, respectively for comparison (●). The average peak IPSCs evoked by photostimulation in the reticular neurons ( $90 \pm 21 \text{ pA}$ , red triangles) were significantly smaller than the average IPSCs of the relay neurons in both cases (Fig. 3*C*:  $517 \pm 54 \text{ pA}$ ,  $t = 6.30$ ,  $P < 0.0001$ ; Fig. 3*D*:  $244 \pm 35 \text{ pA}$ ,  $t = 3.37$ ,  $P < 0.005$ ; red circles), even though higher laser powers were used for the reticulo-reticular stimulation.

#### Effects of TTX on photostimulation responses

Electron microscopic examination of the thalamic reticular nucleus has suggested the presence of dendrodendritic synapses between reticular neurons (Deschênes et al. 1985; Pinault et al. 1997; Yen et al. 1985). Dendrodendritic synapses also exist in the lateral geniculate nucleus between the dendrites of interneurons and relay cells in the rat and cat (reviewed in Jones 1985; Sherman and Guillery 2006). Those synapses can be activated in the presence of TTX, implying that action potentials are not needed to produce transmitter release, provided local depolarization of the presynaptic element occurs (Cox and Sherman 2000; Lam et al. 2005). We sought to determine whether dendrodendritic synapses in the thalamic reticular nucleus could also be activated in the presence of TTX. Figure 4 shows our ability to observe TTX-independent IPSCs in relay cells of the lateral geniculate nucleus using photostimulation. Geniculate neurons were recorded in voltage-clamp mode and photostimulated at 128 positions in an  $8 \times 16$  array (Fig. 4, middle) roughly centered on the recording site. Photostimulation evoked a late outward (hyperpolarizing) current that was not completely blocked by  $1 \mu\text{M}$  TTX (Fig. 4, right). Selected traces are also shown in larger scale (Fig. 4, left). A similar TTX-independent outward current was observed in all five geniculate neurons tested. In the context of our earlier studies of this effect, we interpret these outward currents as GABAergic IPSCs derived from the dendrodendritic F2 terminals.

In contrast to IPSCs evoked from geniculate relay cells, the IPSCs evoked in reticular neurons by reticular photostimulation were totally blocked (or undetectable) after bath-application of  $1 \mu\text{M}$  TTX. Figure 5 shows the result of one such experiment, and here the photomicrograph of the slice and

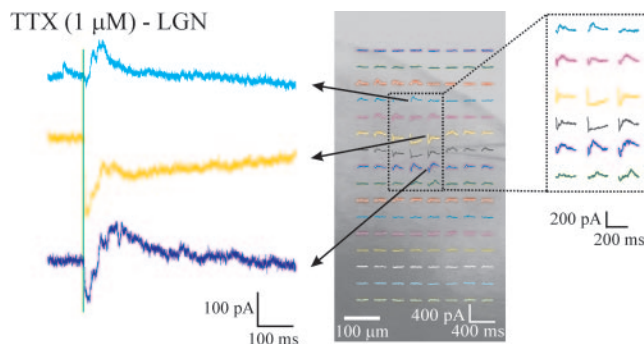


FIG. 4. Photostimulation evoked TTX-insensitive responses in relay cell of the lateral geniculate nucleus. Recordings are in voltage-clamp mode, and the laser power was 19 mW. Columnar organization as in Fig. 2. A biphasic depolarization/hyperpolarization response could be elicited by photostimulation in the presence of  $1 \mu\text{M}$  TTX.

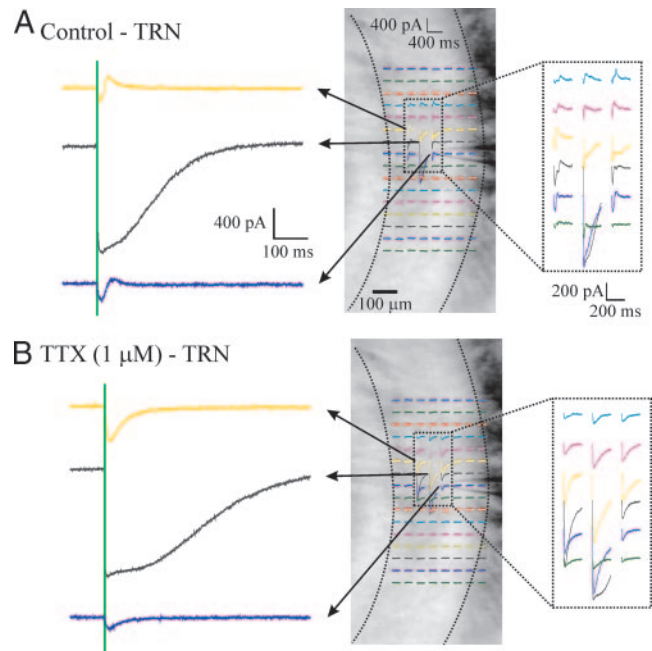


FIG. 5. Photostimulation evoked responses of reticular cell in the presence of TTX. Recordings are in voltage-clamp mode, and laser power was 21 mW. Columnar organization as in Fig. 2. Dotted lines indicate location of thalamic reticular nucleus. *A*: control, showing biphasic depolarization/synaptic response. *B*: application of  $1 \mu\text{M}$  TTX abolishes outward (hyperpolarizing) current, which is the synaptic component of response.

responses to photostimulation at 128 locations are shown in the middle. Response traces evoked by photostimulation in the area immediately surrounding the soma are shown in larger scale on the right, and selected full traces are shown on the left. Figure 5*A* shows the responses before, and Fig. 5*B* after, the addition of  $1 \mu\text{M}$  TTX. In this and four other experiments, we could not detect any hyperpolarization component after the TTX was applied.

#### Reponses through electrical synapses

In 8 of the 47 experiments, we observed sharp depolarizing spikelets characteristic of electrical synapses in addition to the slower direct depolarizing and hyperpolarizing responses. Figure 6 shows voltage-clamp recordings from an example in which the IPSCs were blocked by SR95531. A photomicrograph and 200-ms traces after photostimulation show the spatial extent in which the spikelets could be evoked (Fig. 6, middle and right), and this extent, which is similar to the evoked region for direct depolarization and evoked IPSCs, consisted of a small elliptical area around the recorded neuron. Figure 6*A* shows the unfiltered traces, and Fig. 6*B* shows the spikelets more clearly after the traces were high-pass filtered. We tested the effects of the gap-junction blocker, carbenoxolone, on the spikelets in two experiments. Bath application of  $200 \mu\text{M}$  carbenoxolone completely inhibited the spikelets without any effect on the hyperpolarization component from GABAergic synapses (Fig. 7, right).

#### DISCUSSION

We used laser-scanning photostimulation to study the interconnections between neurons of the thalamic reticular nucleus.

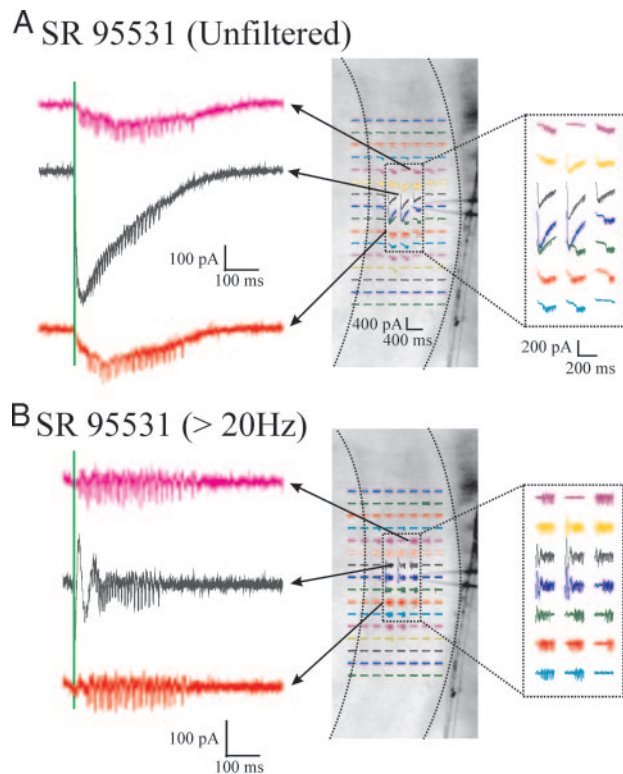


FIG. 6. Evidence for gap junctions between reticular cell. Recordings were performed in voltage-clamp mode, and laser power was 10 mW. Columnar organization as in Fig. 2. Dotted lines indicate location of thalamic reticular nucleus. *A*: photostimulation in area around soma of a reticular cell evoked fast depolarizing spikelets characteristic of gap junctions. *B*: high-pass filtering of traces to show spikelets more clearly.

In comparison with the more traditional means of electrical stimulation, this technique of neuronal activation has the advantages that fibers of passage are not activated and that strong stimuli can be delivered in spatially precise patterns. We were able to document connections between nearby reticular neurons, both chemical (GABAergic) and electrical, and estimated the strength and spatial extent of these interconnections. We also showed that the GABAergic connections between reticular cells are weaker than those from reticular to relay cells.

Our experiments were conducted using young animals (10–12 days of age), because the poor visibility in slices from older animals impairs visualization and thus compromises successful patch-clamp recording. It is plausible that the animal's age could affect the size of the dendritic and axonal arbors of reticular neurons and thus the spatial extent by which they interconnect, but histological studies of neurons from the adult rat's thalamic reticular nucleus (Pinault et al. 1995a,b) do not indicate dramatically different dendritic structures from what we observed in our experiments. Electrical synapses are reported to persist in adult animals (Long et al. 2004), although quantitative comparisons of their distribution across stages of development are unavailable. It is therefore possible that the relative importance of chemical and electrical synapses could change with age.

#### GABAergic connections

CONNECTIONS BETWEEN RETICULAR CELLS. Our data indicate that reticular neurons are interconnected predominately

through GABAergic axodendritic synapses. We detected GABAergic IPSCs in 29 of 47 recorded reticular neurons. This number could be an underestimate for several reasons. For instance, there is always the possibility that some of the connections between cells are severed in the slice; also, small IPSCs could be easily concealed by the large depolarization evoked directly from photostimulation.

We have also tried the experiment without using  $\text{Cs}^+$  in the recording pipette to detect  $\text{GABA}_B$  responses. In such cases, we were able to completely block the evoked IPSCs with antagonists to the  $\text{GABA}_A$  receptor and thus were unable to show a  $\text{GABA}_B$  response component (data not shown). Although negative results are hard to interpret, the fact that, using similar techniques, we readily evoked  $\text{GABA}_B$  responses in the reticular to relay cell pathway adds weight to this negative result. Nonetheless, Sanchez-Vives et al. (1997) did report  $\text{GABA}_B$  response components in IPSCs elicited between cells of the ferret's perigeniculate nucleus, which is regarded as a region of the thalamic reticular nucleus. This difference in  $\text{GABA}_B$  response may be caused by species or nuclear differences or it may well reflect a false negative in our data. That is, perhaps the  $\text{GABA}_B$  response was simply too small to be detected using our methods or activation of reticulo-reticular  $\text{GABA}_B$  responses might require a much higher rate of firing among reticular cells than could be activated by the photostimulation we employed (however, see Fig. 1).

We were able to provide a spatial map of the synaptic connections between reticular neurons (Fig. 2). Each reticular neuron receives inhibitory input from its neighbors in an area of only  $\sim 350 \times 200 \mu\text{m}$ . This area is similar to the size of the dendritic arbors of reticular cells we labeled with biocytin (data not shown). It is also consistent with anatomical data indicating that axon collaterals of reticular cells extend for a short distance within the thalamic reticular nucleus (Cox et al. 1996; Liu and Jones 1999). It is possible that axons cut in the slice reduced the effective afferent area somewhat, but we did find comparable afferent areas with both slice orientations used (22 horizontal and 7 thalamocortical slices).

COMPARISON WITH RETICULO-THALAMIC CONNECTIONS. We used the same techniques to study IPSCs in relay cells evoked by reticular photostimulation (Lam and Sherman 2005). We measured and averaged the peak values of the IPSCs evoked by photostimulation on both sides  $\sim 100 \mu\text{m}$  mediolaterally from the recording site, where the IPSCs were large and the direct

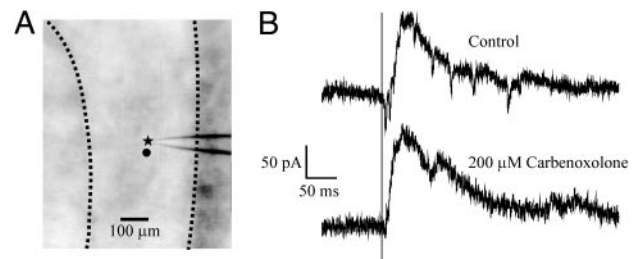


FIG. 7. Inhibition of spikelets by gap-junction antagonist. Recordings are in voltage-clamp mode, and laser power was 16 mW. Dotted lines indicate location of thalamic reticular nucleus. *A*: photomicrograph of slice. Soma of the reticular cell is indicated with a star, and site of photostimulation, with a closed circle. *B*: top trace shows that photostimulation induced an outward synaptic current (hyperpolarizing) and fast, multiple spikelets. Bottom trace shows that application of gap-junction antagonist, carbenoxolone ( $200 \mu\text{M}$ ), blocks spikelets without any effect on synaptic response.

depolarization was relatively small (Fig. 3A). These values were compared with the maximum IPSCs evoked in relay cells by photostimulation at the centroid of their reticular input footprint (Fig. 3C). We found that the IPSCs evoked in reticular cells were much smaller than those in relay cells, even when the laser power was higher (Fig. 3C). We also considered the possibility that the IPSCs evoked 100  $\mu\text{m}$  medio-lateral from the recording site might not reflect the full strength of reticulo-reticular synapses. We therefore compared the reticulo-reticular IPSCs to the reticulo-relay cells IPSCs evoked 100  $\mu\text{m}$  medio-lateral from the centroid of their reticular input footprint. Again, the reticulo-relay cells IPSCs were larger despite the lower laser powers used (Fig. 3D).

Two other factors might also work against this difference: first, the longer distance in the reticulo-thalamic path means a greater chance of severing axons; and second, reticular synapses on relay cells are on distal dendrites, which might reduce their impact at the soma, although we do not know where reticulo-reticular synapses are located.

Strictly speaking, because photostimulation only excites presynaptic neurons within a limited illuminated region, presynaptic cells that are scattered about as opposed to clustered spatially would be interpreted as possessing a "weaker" set of connections. It is therefore theoretically possible that our results can be explained simply by the reticulo-relay cell connections being spatially more concentrated than the inhibitory connections within the thalamic reticular nucleus. This scenario, however, is unlikely because it would require that reticulo-reticular IPSCs can be evoked in a much larger area than the reticulo-relay cells (IPSCs). We did not see such difference.

The difference of synaptic strength could be explained by a smaller number of functional synapses, as suggested by anatomic observations (Cox et al. 1996; Scheibel and Scheibel 1966; Yen et al. 1985) and/or weaker synapses (Zhang et al. 1997). A similar difference in synaptic strength was reported for the IPSCs in relay cells and reticular neurons evoked by bipolar electrodes, using minimal stimulation, although it was suggested that the weaker synapses between reticular neurons could be compensated by the slow decay time of their IPSCs (Zhang et al. 1997). Data shown here indicate that when a larger (and probably more biological) number of reticular neurons were activated using photostimulation, the difference between the two pathways is even more pronounced.

**DENDRODENDRITIC SYNAPSES.** Electron microscopic examination of the thalamic reticular nucleus has suggested the presence of dendrodendritic synapses between reticular neurons (Deschênes et al. 1985; Pinault et al. 1997; Yen et al. 1985). Similar synapses between interneurons and thalamic relay cells in the lateral geniculate nucleus can be activated by photostimulation in the presence of TTX (Fig. 4), suggesting action potentials are not needed for GABAergic release, and this GABA release seems to result from the direct activation of the dendrodendritic terminals by uncaged glutamate molecules (Cox and Sherman 2000; Lam et al. 2005). In contrast, the response evoked in reticular neurons by local photostimulation is completely blocked by TTX (Fig. 5). There are several possible explanations for this. 1) The dendrodendritic synapses between reticular neurons are very weak and hard to detect functionally. 2) They require a much larger depolarization for

activation, perhaps involving back-propagation of action potentials, than we can deliver with TTX present. 3) There are no glutamate receptors near these synapses to produce a sufficiently large local depolarization through photostimulation; we know, for example, that the presynaptic dendritic terminal in the lateral geniculate nucleus does have glutamatergic receptors (Cox and Sherman 2000; Godwin et al. 1996).

### *Electrical synapses*

Because photostimulation depolarizes (presynaptic) reticular neurons strongly and evokes a long train of action potentials (Fig. 1), electrical synapses can be detected by the depolarizing spikelets in the response of reticular neurons to photostimulation (Fig. 6). The specific inhibition of these spikelets by a gap-junction blocker further confirms their electrical nature (Fig. 7). We detected such responses indicative of electrical synapses in 8 of 47 neurons (17%). The percentage is smaller though roughly comparable with that revealed from paired recording of rat reticular neurons (31%; Landisman et al. 2002). We found electrical synapses only between neighboring reticular neurons, in agreement with previous results (Landisman et al. 2002; Long et al. 2004). An important difference between studies, however, is that our data indicate a large proportion of reticular neurons receive axodendritic synaptic inputs from other reticular neurons, whereas Landisman et al. (2002) could not find pairs connected with detectable chemical synapses. This may simply mean that photostimulation, which activates a group of inputs to a cell can thus provide a larger combined IPSC, whereas the IPSC from input from a single neuron during paired recording is too small to be detected.

### *Functional implications*

Our main conclusion is that reticular cells receive a relatively weak GABAergic input from nearby neighbors. The obvious implication is that a strong activation of a focus of reticular neurons will produce a surrounding region of mild inhibition. Because reticular cells inhibit relay cells, strong activation of a focal region of reticular cells would serve to disinhibit their target relay cells. To fully understand the implication of this, we need a more detailed understanding of the connections between relay and reticular cells in both directions.

Our previous study of the reticulo-thalamic limb of this system (Lam and Sherman 2005) indicates that the afferent footprint has a relatively simple structure with increasing strength of connection near its center. One might thus imagine that any strong focus of activation of a group of reticular cells would produce an area of reticular activity that, in turn, would inhibit relay cells. The presence of local, reticulo-reticular inhibition would serve to sharpen the focus of the activated reticular zone, and in this sense, the pattern of reticular interconnectivity we have described may serve to sharpen functional connections in the reticulo-thalamic pathway.

### GRANTS

This research was supported by National Eye Institute Grant EY-03038 to S. M. Sherman and a Howard Hughes Undergraduate Fellowship to C. S. Nelson.



## REFERENCES

- Agmon A and Connors BW.** Thalamocortical responses of mouse somatosensory (barrel) cortex in vitro. *Neuroscience* 41: 365–379, 1991.
- Canepari M, Nelson L, Papageorgiou G, Corrie JE, and Ogden D.** Photochemical and pharmacological evaluation of 7-nitroindolyl- and 4-methoxy-7-nitroindolyl-amino acids as novel, fast caged neurotransmitters. *J Neurosci Methods* 112: 29–42, 2001.
- Cox CL, Huguenard JR, and Prince DA.** Heterogeneous axonal arborizations of rat thalamic reticular neurons in the ventrobasal nucleus. *J Comp Neurol* 366: 416–430, 1996.
- Cox CL and Sherman SM.** Control of dendritic outputs of inhibitory interneurons in the lateral geniculate nucleus. *Neuron* 27: 597–610, 2000.
- Crabtree JW.** The somatotopic organization within the cat's thalamic reticular nucleus. *Eur J Neurosci* 4: 1352–1361, 1992a.
- Crabtree JW.** The somatotopic organization within the rabbit's thalamic reticular nucleus. *Eur J Neurosci* 4: 1343–1351, 1992b.
- Crabtree JW.** Organization in the somatosensory sector of the cat's thalamic reticular nucleus. *J Comp Neurol* 366: 207–222, 1996.
- Deschênes M, Madariaga-Domich A, and Steriade M.** Dendrodendritic synapses in the cat reticularis thalami nucleus: a structural basis for thalamic spindle synchronization. *Brain Res* 334: 165–168, 1985.
- Fuentealba P and Steriade M.** The reticular nucleus revisited: intrinsic and network properties of a thalamic pacemaker. *Prog Neurobiol* 75: 125–141, 2005.
- Godwin DW, Van Horn SC, Eri'ir A, Sesma M, Romano C, and Sherman SM.** Ultrastructural localization suggests that retinal and cortical inputs access different metabotropic glutamate receptors in the lateral geniculate nucleus. *J Neurosci* 16: 8181–8192, 1996.
- Guillery RW, Feig SL, and Lozsádi DA.** Paying attention to the thalamic reticular nucleus. *Trends Neurosci* 21: 28–32, 1998.
- Guillery RW and Harting JK.** Structure and connections of the thalamic reticular nucleus: advancing views over half a century. *J Comp Neurol* 463: 360–371, 2003.
- Jones EG.** *The Thalamus*. New York: Plenum Press, 1985.
- Lam YW, Cox CL, Varela C, and Sherman SM.** Morphological correlates of triadic circuitry in the lateral geniculate nucleus of cats and rats. *J Neurophysiol* 93: 748–757, 2005.
- Lam YW and Sherman SM.** Mapping by laser photostimulation of connections between the thalamic reticular and ventral posterior lateral nuclei in the rat. *J Neurophysiol* 94: 2472–2483, 2005.
- Landisman CE and Connors BW.** Long-term modulation of electrical synapses in the mammalian thalamus. *Science* 310: 1809–1813, 2005.
- Landisman CE, Long MA, Beierlein M, Deans MR, Paul DL, and Connors BW.** Electrical synapses in the thalamic reticular nucleus. *J Neurosci* 22: 1002–1009, 2002.
- Liu XB and Jones EG.** Predominance of corticothalamic synaptic inputs to thalamic reticular nucleus neurons in the rat. *J Comp Neurol* 414: 67–79, 1999.
- Long MA, Landisman CE, and Connors BW.** Small clusters of electrically coupled neurons generate synchronous rhythms in the thalamic reticular nucleus. *J Neurosci* 24: 341–349, 2004.
- Pinault D.** The thalamic reticular nucleus: structure, function and concept. *Brain Res Rev* 46: 1–31, 2004.
- Pinault D, Bourassa J, and Deschênes M.** Thalamic reticular input to the rat visual thalamus: a single fiber study using biocytin as an anterograde tracer. *Brain Res* 670: 147–152, 1995a.
- Pinault D, Bourassa J, and Deschênes M.** The axonal arborization of single thalamic reticular neurons in the somatosensory thalamus of the rat. *Eur J Neurosci* 7: 31–40, 1995b.
- Pinault D, Smith Y, and Deschênes M.** Dendrodendritic and axoaxonic synapses in the thalamic reticular nucleus of the adult rat. *J Neurosci* 17: 3215–3233, 1997.
- Reichova I and Sherman SM.** Somatosensory corticothalamic projections: distinguishing drivers from modulators. *J Neurophysiol* 92: 2185–2197, 2004.
- Sanchez-Vives MV, Bal T, and McCormick DA.** Inhibitory interactions between perigeniculate GABAergic neurons. *J Neurosci* 17: 8894–8908, 1997.
- Scheibel ME and Scheibel AB.** The organization of the nucleus reticularis thalami: a Golgi study. *Brain Res* 1: 43–62, 1966.
- Shepherd GM, Pologruto TA, and Svoboda K.** Circuit analysis of experience-dependent plasticity in the developing rat barrel cortex. *Neuron* 38: 277–289, 2003.
- Sherman SM and Guillery RW.** *Exploring the Thalamus and Its Role in Cortical Function*. Cambridge, MA: MIT Press, 2006.
- Shu YS and McCormick DA.** Inhibitory interactions between ferret thalamic reticular neurons. *J Neurophysiol* 87: 2571–2576, 2002.
- Yen CT, Conley M, Hendry SHC, and Jones EG.** The morphology of physiologically identified GABAergic neurons in the somatic sensory part of the thalamic reticular nucleus in the cat. *J Neurosci* 5: 2254–2268, 1985.
- Zhang SJ, Huguenard JR, and Prince DA.** GABA<sub>A</sub> receptor-mediated Cl<sup>-</sup> currents in rat thalamic reticular and relay neurons. *J Neurophysiol* 78: 2280–2286, 1997.